Towards a semi-active vibration control solution based on superelastic shape memory alloys

C. Cismasiu & F. P. Amarante dos Santos
Centro de Investigação em Estruturas e Construção - UNIC, Faculdade de Ciências e Tecnologia, Universidade Nova de Lisboa, 2829-516, Caparica, Portugal

SUMMARY:
The paper presents a novel semi-active control device based on superelastic NiTi wires working in phase opposition. Its design avoids problems related to stress-relaxation and material degradation due to cyclic loading, which have been observed in similar passive dissipation devices. The functioning principle of the device is given and numerical simulations based on a constitutive model, calibrated with experimental tests, are used to confirm its efficiency under seismic excitations. As to confirm experimentally the numerical results and to assess the performance of the proposed control system, a small scale physical prototype that simulates the response of a single degree of freedom dynamic system equipped with the proposed semi-active vibration control device is built and tested under harmonic excitation using a shake table.

Keywords: superelastic SMA wires; semi-active vibration control; small scale physical prototype.

1. INTRODUCTION

Superelasticity, a peculiar thermo-mechanical property of shape memory alloys (SMAs), allows the material to recover from large nonlinear strains during a mechanical cycle of loading and unloading, while dissipating a considerable amount of energy through hysteresis. Exploiting this property, several authors report on successful implementations of SMAs in passive vibration control devices, especially designed for seismic hazard mitigation [1, 2, 3, 4, 5, 6, 7]. Most of these devices are built up of Nitinol (NiTi), a dual alloy built up of Nickel and Titanium, due to its outstanding fatigue properties, high corrosion resistance and ductility.

The vibration control device proposed in the present work, originates from the NiTi based passive dissipation device reported by Dolce *et al.* [1]. As to increase its energy dissipation capabilities, the original device was made of sets of pretensioned wires working in phase opposition. However, a variety of relaxation phenomena observed in pretensioned SE wires [8, 9] might have an adverse impact on the dynamic performances of the device. Mainly to avoid these problems, the proposed semi-active device uses a strategy that allows the continuous adapting of the accumulated strain in the wires, based on the response of the device to external excitations. As in an active control system, a controller monitors the feedback measurements and generates appropriate command signals for the device. As in a passive control system however, the control forces are developed as a result of the motion of the structure itself, with no need of external energy input. As the control forces act as to oppose the motion of the structural system, they promote the global stability of the structure [10]. According to presently accepted definitions [11], the proposed device may be considered as a semi-active control system.

2. ADOPTED CONSTITUTIVE MODEL

The behaviour of SMAs is highly complex, as it depends on stress and temperature and is closely

connected with the crystallographic phase of the material and the thermodynamics underlying the transformation processes. While strain or stress rate independent models [12, 13, 14] may be well suited for quasi-static analysis when isothermal conditions may be assumed, for most dynamic applications, rate dependent models are usually required, due to self-heating [15, 16, 17]. A common features present in most of these models, is the presence of a distinct mechanical law, governing the stress-strain relations, and of a kinetic law, governing the martensitic transformations. The mechanical law relates the stress, strain, temperature and martensite fraction. The martensite fraction represents the extent of the transformed phase, which is considered to be in series with the elastic fraction. According to the literature [18], there are several possible approaches to model the elastic component: the simple serial model, the Voight and the Reuss schemes. The transformation kinetic laws describe mathematically the evolution of the martensite fraction with stress and temperature, based on the material's stress-temperature phase diagram. Several kinetic laws are available in the literature, ranging from linear [19] or exponential laws [15], to cosine based kinetic laws [16] and thermodynamically derived relations [17]. In the case of rate dependent models, to conveniently model the thermal effects, a heat balance equation is coupled with the mechanical and kinetic transformation laws.

The adopted rate-dependent constitutive model is based on Tanaka's temperature dependent model [15]. In order to relate stress, strain, temperature and martensite fraction in the material, the model couples the constitutive relations to an exponential kinetic law that describes the volume fraction of austenite [20]. When associated to a balance equation that considers the thermal effects on the material, this constitutive model produces reliable results even for high strain rates [21, 22].

3. THERMO-MECHANICAL PROPERTIES

In order to characterise the NiTi tensile behaviour, a Differential Scanning Calorimetry thermo-analytical analysis and a set of quasi-static tensile tests at different ambient temperatures have being carried out on NiTi SE508 wire specimens, with 2.4 mm diameter and circular cross section, provided by Euroflex GmbH. These experimental tests, described in more detail in [23, 24], yield the values in Table 1 for the austenitic and martensitic elastic modulus, E_A and E_M, the four transformation temperatures, M_s and M_f during cooling and A_s and A_f during heating, the Clausis-Clapeyron coefficient, assumed to be the same for the forward C_M and inverse C_A transformations and the maximum residual strain ε_L. For the Poisson's ratio, a typical value of 0.33 is adopted from the literature [25]. To completely characterise the constitutive model, values for several thermophysical properties, like density ρ, latent heat c_L, specific heat c_p, convection coefficient h, thermal expansion coefficient θ and thermal conductivity k, are taken from literature [21].

Table 1. Parameters for adopted constitutive model

E_A = 35000 MPa	E_M = 20000 MPa	M_f = -45 ºC
M_s = -35 ºC	A_s = -15 ºC	A_f = -5 ºC
C_M = 6.5 MPa K^{-1}	C_A = 6.5 MPa K^{-1}	ε_L = 3 %
ρ = 6500 kg m^{-3}	c_L = 12914 J kg^{-1}	c_L = 500 J kg^{-1} K^{-1}
h = 35 W m^{-2} K^{-1}	θ = 6 × 10-6 K^{-1}	k = 18 W m^{-2} K^{-1}

4. NUMERICAL ASSESSMENT OF THE ADOPTED CONSTITUTIVEMODEL

The results of a large set of experimental cyclic tensile tests clearly illustrating the sensitivity of the NiTi wires' mechanical response to temperature and strain rate are used to assess the performances of the constitutive model. For illustration purposes, the experimental curves obtained at 20ºC ambient temperature for strain rates of 0.008 and 0.333%/s are presented in Figure 1 against simulated estimates. These plots clearly illustrate that the implemented rate-dependent numerical model yields sets of very satisfying results, both for the temperature time histories and their corresponding stress-

strain diagrams. It can be seen that, as the strain rate of the dynamic loading increases from 0.008 to 0.333%/s, the simulation predicts increasing changes in the sample temperature during the loading cycle, in close agreement with the experimental data. In what concern the stress-strain diagram, the shape of the hysteretic loops tends to become steeper and narrower with the increase in the strain rate, again in conformity with the trend observed in the experimental tests.

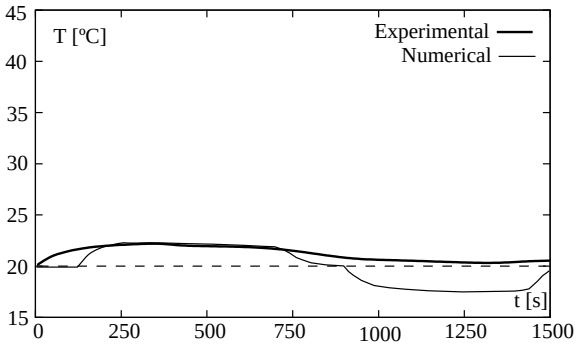

(a) Temperature time history: strain rate 0.008%/s

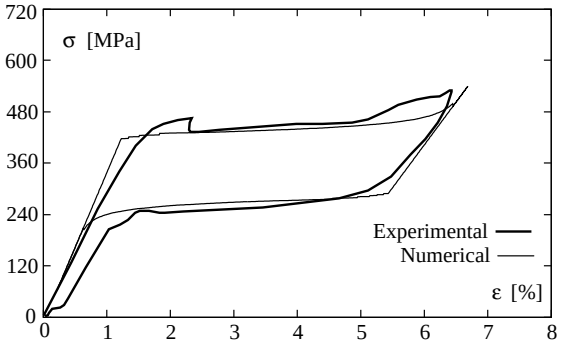

(b) Stress-strain diagram: strain rate 0.008%/s

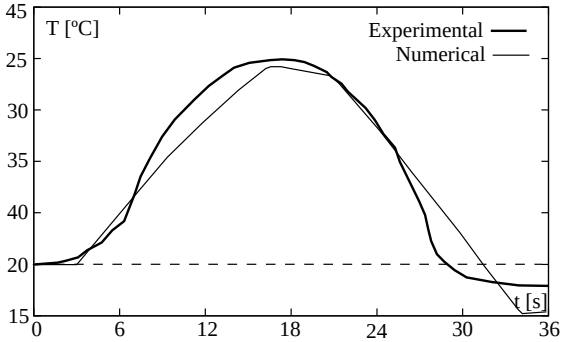

(c) Temperature time history: strain rate 0.333%/s

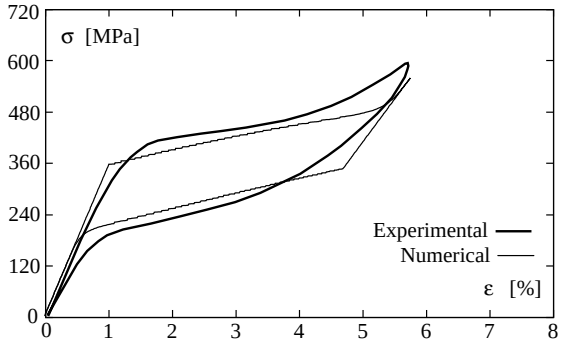

(b) Stress-strain diagram: strain rate 0.333%/s

Figure 1. Dynamic experimental tests: numerical model versus experimental data

5. PROPOSED SEMI-ACTIVE VIBRATION CONTROL DEVICE

The proposed semi-active control device, whose generic functional scheme is given in Figure 2(b), is based on the passive system illustrated in Figure 2(a), being built up of two SE wires working in phase opposition. In passive systems of this type, the wires are connected to the mass and act as restoring elements [1, 4, 22].

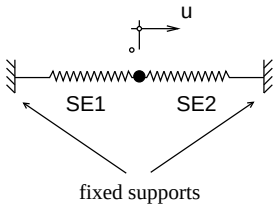

(a) Passive system

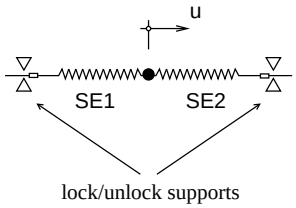

(b) Semi-active system

Figure 2. Generic functional scheme of the passive and the semi-active systems

It is recalled that, in the case of passive systems, a common technique to enhance damping is to enforce a pre-strain in the SE wires [1]. However, this solution is hindered by problems related to

stress relaxation [26] and cumulative creep [5], that do not have a simple solution in a passive device configuration. Stress relaxation can not be avoided, as the use of permanent pre-strained SE wires is a must in order to obtain competitive damping ratios. The cumulative creep can be avoided by keeping the strains inside the recoverable limits of a so called pseudo-elastic window (PEW) [27, 28]. However, this is a very challenging task when dealing with arbitrary seismic excitation.

The proposed semi-active control device minimises the SMA rheological effects by controlling the strain in the SE wires. The strain is self-adjusting, allowing the wires to become strain/stress free, when not subjected to a dynamic excitation. The system is also able to keep the wires deformation inside a given PEW, while guaranteeing a minimal threshold to their strain level. The strain in the SE wires is calibrated by controlling the displacements of the wires at their supports. The two wire supports can assume, independently, two configurations, locked or unlocked. By default, the supports are locked, assuring the adequate restraining for the SE wires. If the system needs to compensate for an excessively low or high strain in a given wire, it momentarily unlocks the wire with a controlled velocity and without introducing additional forces into the system. As the actuating elements only have two fixed positions, this type of control system is usually referred to as a two-position or on-off controller.

5.1. Functioning of the proposed semi-active system

The sequence of actions taken by the semi-active system during a dynamic excitation is explained in Figure 3, which illustrate a typical displacement time-history response to an harmonic excitation.

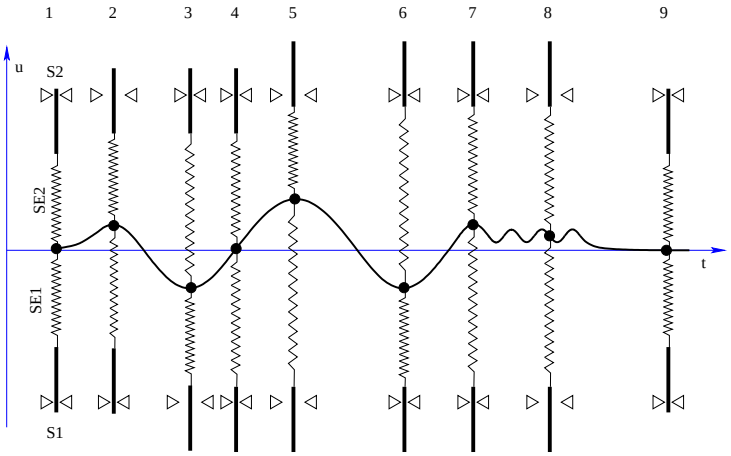

Figure 3. Functioning of the proposed semi-active control system

Initially, the system is resting in its original equilibrium position, referred as position 1 in the figure, with both SE wires, SE1 and SE2, strain/stress free and their supports, S1 and S2, locked. Once the harmonic excitation is applied to the system, the mass starts to move (assume) upwards and the straining of SE1 begins. During the first half cycle of the movement, between position 1 and 2, S2 is unlocked to prevent compression in the corresponding wire, while the support of SE1 is kept locked to ensure the straining of the wire. As the mass reverses its direction, S2 switch to locked, to ensure the straining of SE2. As the movement continues downwards, the support of SE1 remains locked as well, until the mass reaches its original equilibrium position. With this configuration, displacements below this point would cause compression in the SE1. For this reason, as soon as this happens, S1 switches to unlocked, until position 3, when the mass reverses once again its movement. At the end of the first loading cycle, position 4, both SE wires have already accumulated a certain level of strain. Between positions 4 and 5, assuming that in the last one occurs the maximum displacement amplitude, both supports will switch from locked to unlocked: S2, as the strain in SE2 approaches zero to avoid compression, and S1, as the strain in SE1 goes beyond the defined value inside the PEW, preventing it from further straining. If, during an eventual steady state forced vibration phase, positions 5 to 6, there is no need for adjustments in the SE wires to compensate low or high strains, both supports remain

locked. As soon as the dynamic excitation ceases, position 7, the amplitude of the free vibrations starts gradually to diminish because of the SE damping. The system reaches it's steady state free vibration phase, position 8, oscillating around an equilibrium position different from it's original one. During this period, both supports remain locked. At this point, to recover the original equilibrium position, the system unlocks both of the cables, relinquishing the accumulated strain in the wires. Finally, position 9, the supports are locked again to prepare the device for the next dynamic excitation. Note that, every time the system needs to unlock a support, the wire is released with a controlled velocity, which can be seen as a design parameter of the proposed semi-active device.

5.2. Semi-active control device under seismic excitation

Studies on the efficiency of SMA based passive control devices in the context of seismic loading were reported in [22], considering a simplified numerical model of one segment of the São Martinho railway viaduct. For the longitudinal analysis, the segment was assimilated to an elastic, one degree-of-freedom dynamic system, with 4650 ton mass, stiffness of 355×10^3 kN/m and 5 % structural damping. The records of two historic strong earthquakes, *El Centro* and *Kobe*, as provided by the Pacific Earthquake Engineering Research Center and the University of California in the PEER Strong Motion Database [29], are used in the numerical simulation.

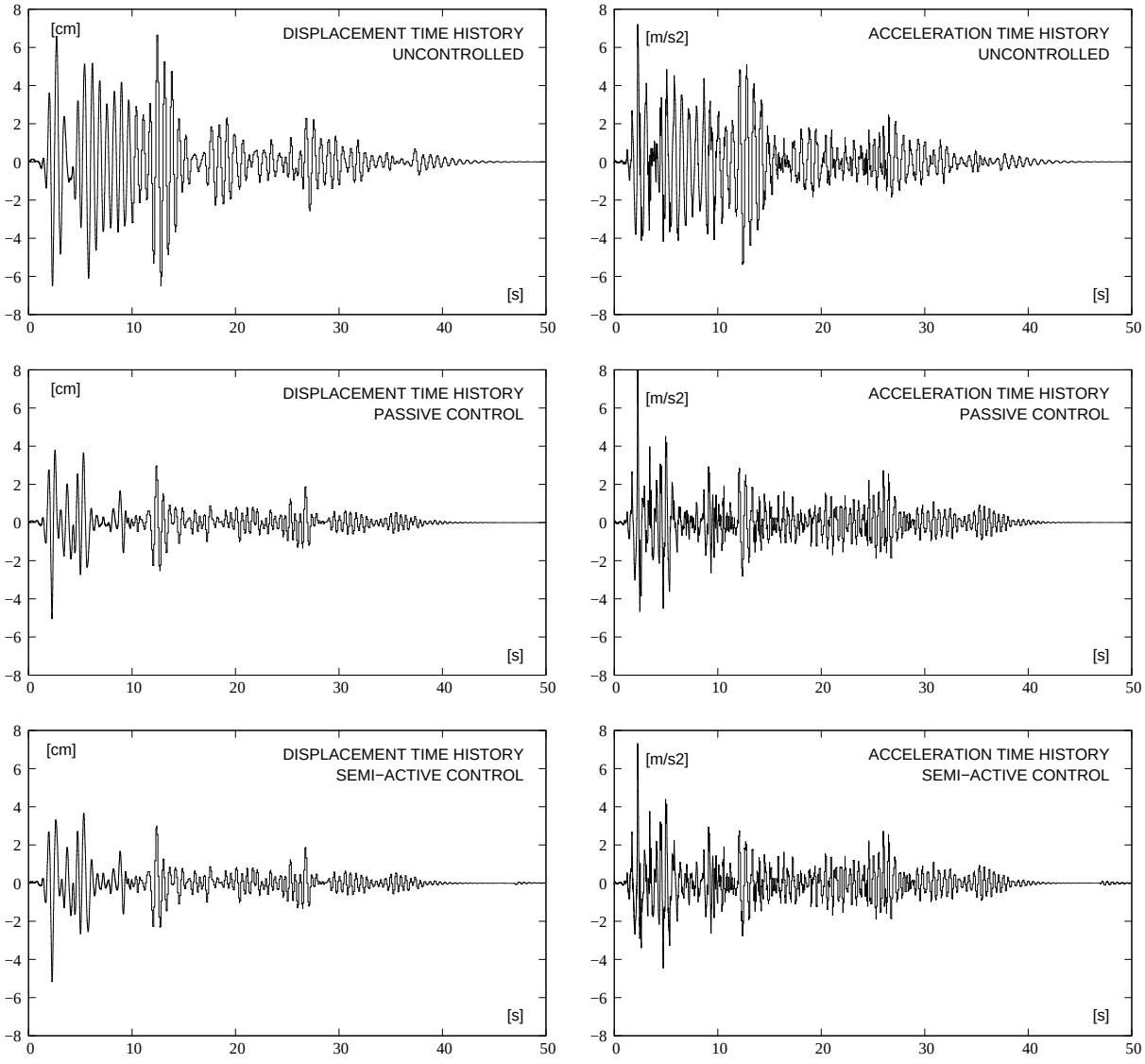

Figure 4. *El Centro*: displacement and acceleration time history for the free and controlled structure

To emphasise the benefits of the proposed semi-active control device on the structural response of the viaduct, three cases are considered: the uncontrolled structure, the structure controlled with a SMA based passive device and the structure controlled with the semi-active device. Note that, in order to get comparable sets of results, the strain level in the SE wires of the passive device was set equal with the maximum strain level attained in the semi-active device. To obtain an adequate response of the semi-active device to the higher frequency content of the seismic action, when the supports are unlocked, the wires are released with a velocity of 1 m/s. Two control devices, both either passive either semi-active, are placed at the ends of the viaduct segment. Each of them is composed of two sets of 1 m SMA wires, each set with a total area of 100 cm^2. This section could be built up of bars or a set of smaller wires laid parallel in strands, to form a cable. The mechanical characteristics of the SMAs are the ones defined in Table 1. A pre-strain of 2.25 % is considered in the passive device, equal to the resulting cumulative strain in the semi-active device.

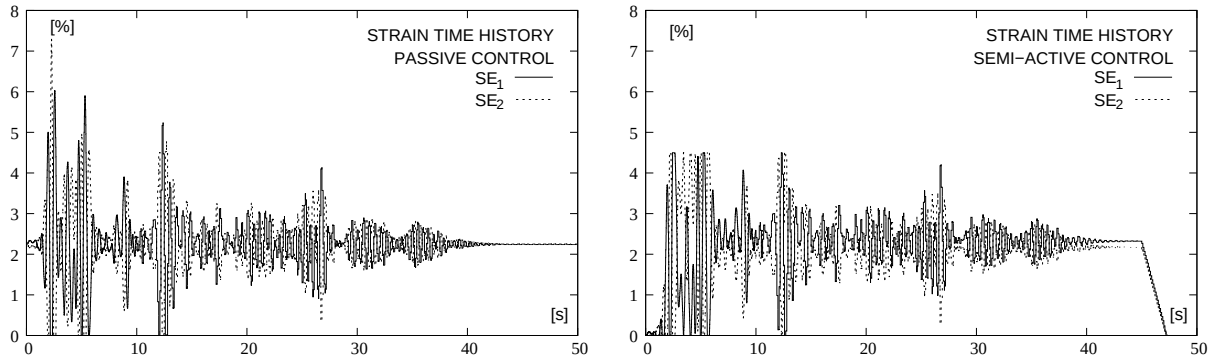

Figure 5. *El Centro*: strain time history in the SE wires of the controlled structure

The displacement and acceleration time histories of the viaduct deck in the longitudinal direction, as well as the strain time history in the SE wires of the passive and semi-active control system, obtained when the structure was subjected to *El Centro* earthquake, are presented in Figures 4 and 5, respectively. Analysing the plots in Figure 4, one can see that the two control devices exhibit similar damping characteristics, being able to considerably reduce the amplitude of the earthquake induced displacements and accelerations. The plots in Figure 5 however, illustrate that the strain time history in the SE wires is quite different for the two adopted control solutions. Although the pre-strain in the passive device is equal to the cumulative strain in the semi-active device, one can see that the maximum strains developed in the passive device are considerably larger when compared with the ones developed in its semi-active counterpart. As their values are outside the PEW, the long term behaviour of the passive device might be compromised. One can observe that, when the seismic excitation stops, the SE wires return to their initial pre-strain, favouring the occurrence of relaxation phenomena. On the other hand, in the semi-active device, the wires return to their strain free condition at the end of the loading.

Therefore, except for the long term relaxation phenomena, the two control solution produce equivalent results. One must note however that, in order to avoid failure in the SE wires, the pre-strain level in the passive control device was calibrated according to the given seismic excitation. A different seismic action applied to the same structure configuration, might produce completely different results. To illustrate this behaviour, the structure is subjected to *Kobe* earthquake. Analysing the dynamical response of the structure presented in Figures 6 and 7, one can see that the passive control device fails, as its SE wires' ultimate strain capacity (≈ 10 - 12%) is exceeded. Besides relaxation and creep potential problems, the fact that these type of solutions need an a priori value for the level of pre-strain in the SE wires, represent an important drawback in the case of seismic applications. While estimates for the maximum strain in the SE wires are relatively easy to obtain in the case of service loads, and therefore a corresponding value for the necessarily pre-strain can be computed, this is no longer the case for extraordinary dynamic loads. With no need of initial pre-strain calibration, its semi-active counterpart responds well to virtually any level of dynamic excitation, as illustrated here in the case of Kobe earthquake. When the response of the structure is compared with the one obtained for the El

Centro earthquake, one can see that the system exhibits similar characteristics. It presents important damping capabilities, is able to confine the strains in the SE wires to predefined levels, inside the PEW, and finally, at the end of the action, is able to recover the SE wires strain free condition. Another benefic aspect related to the semi-active control device is its ability to confine the force values throughout the entire duration of the seismic action, meaning that, when implemented in a civil engineering structure, the force the semi-active device transmits to the structure can be conveniently bounded.

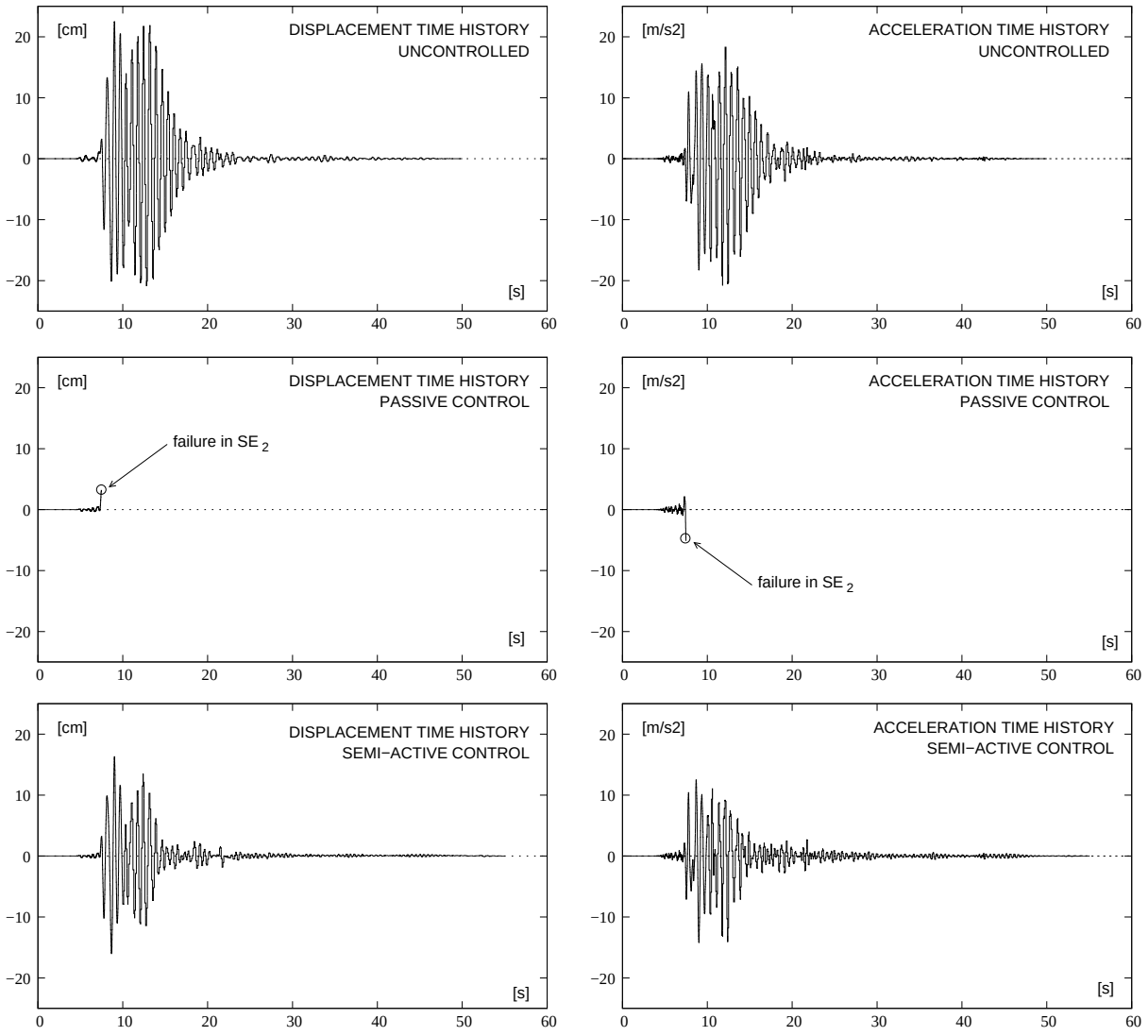

Figure 6. *Kobe*: displacement and acceleration time history for the free and controlled structure

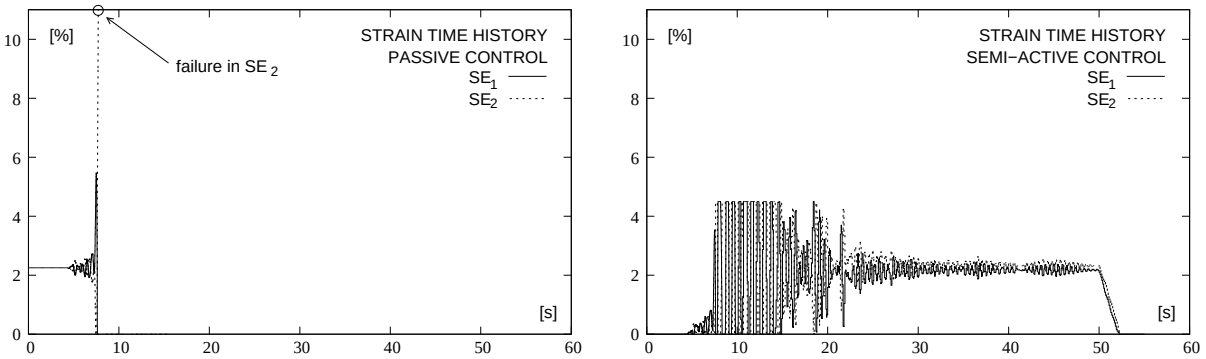

Figure 7. *Kobe*: strain time history in the SE wires of the controlled structure

6. SMALL SCALE PROTOTYPE

To confirm experimentally the conclusions of the numerical simulations and to assess the performance of the semi-active control system, a small scale prototype simulating the response of a single degree of freedom dynamic system equipped with the proposed device is built and tested under harmonic excitation using a Quanser shake table.

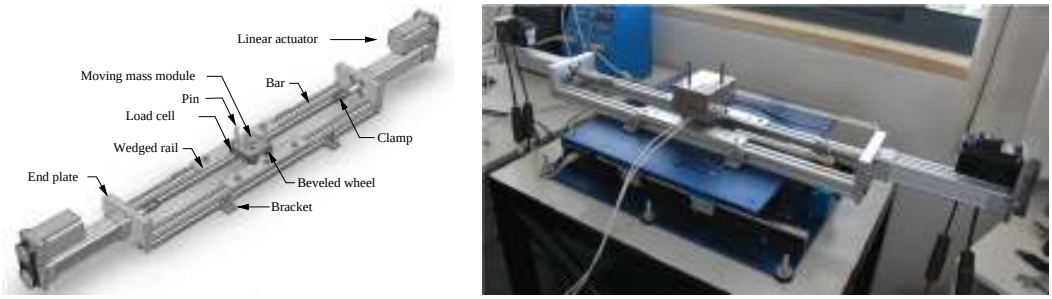

Figure 8. General design concept for the physical prototype

A detailed description of the design and manufacturing of the physical prototype, whose kernel elements are presented in Figure 8, is given in [23, 30]. The prototype, configured for a moving mass of 6.1 kg and two SE NiTi wires with a diameter of 0.406 mm and 0.2 m length, working in phase opposition as restoring elements, is subjected to an harmonic excitation with a frequency of 1 Hz and an amplitude of 5 cm.

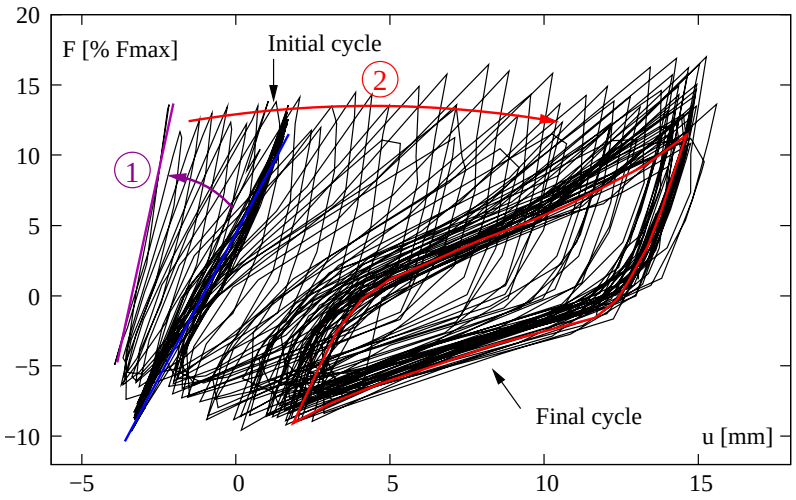

Figure 9. Response of the controlled dynamic system: force-displacement diagram

Analyzing the resulting force-displacement diagram depicted in Figure 9, one can see that the force accumulation in the SE wires, corresponding to an increase of the martensitic transformation, enhances the damping capability of the system.

The dynamic loading starts with the SE wires free of stress/strain and the control system switched off, which means that the device acts like a passive control system with no pre-strain. The SE wires work alternately and because of the relatively small amplitude of the displacements, remain in their austenitic form. This is translated in a linear relation between the total force yielded by the device and the corresponding displacements of the moving mass, the initial cycle in Figure 9.

After 10 seconds of the beginning of the experiment, the control system is switched on and the system rapidly starts to compensate for low stresses in the SE wires. As the total force starts to accumulate, the overall stiffness of the system is increased. This behaviour is identified in Figure 9 by step 1,

during which the slope of the force-displacement curve becomes steeper, since both of the austenitic SE wires start contributing to the system's stiffness. One can see that the martensitic transformation is not initiated yet, and therefore no hysteretic damping is observed.

After this initial stiffening, as the SE wires continue to accumulate force, stress induced martensite starts to develop and the system becomes gradually more flexible. This process is identified in step 2, and leads to the appearance of a stabilised SE hysteretic loop.

The shifting of the center of the loop to the negative displacement region means that the system has sustained a rigid-body movement to the left, with respect it's original position.

7. CONCLUSIONS

The proposed semi-active vibration control device originates from a passive control system, based on SE austenitic wires. In its semi-active version, the system continuously adjusts the strain in the SE wires in order to improve its dynamical characteristics. As the strain accumulation in the wires is a result of the motion of the structure itself, there is no need of external energy input in the system. To avoid relaxation, the SE wires are set strain free at the end of the loading period.

The numerical simulations shows that the system is able to dissipate a considerable amount of energy, while keeping the SE wires inside the recoverable limits defined by the PEW, to minimise the rheological effects related to cumulative creep. It also guarantees a minimal threshold to the strain level in the SE wires to avoid compression and exhibit efficient recentering capabilities.

As to confirm experimentally the numerical results and to assess the performances of the proposed semi-active vibration control device, a small scale physical prototype that simulates the response of a controlled SDOF dynamic system is built and tested under harmonic excitation, induced by a shake table. Analysing the results of these experimental tests, one can conclude that the control device performed adequately as it promotes the force accumulation in the SE wires, enabling the development of a wide SE hysteretic loop and enhance damping.

The reported numerical and experimental simulations clearly demonstrate the potential of the proposed semi-active control device, in improving the seismic response of civil engineering structures.

AKCNOWLEDGEMENT
This work was partially supported by contract SFRH/BD/37653/2007 with FCT/MCTES. Cooperation with Professors F. M. Braz Fernandes and J. Pamies Teixeira from FCT/UNL, is gratefully acknowledged.

REFERENCES

[1] M. Dolce, D. Cardone, R. Marnetto. (2000). Implementation and testing of passive control devices based on shape memory alloys. *Earthquake Engineering and Structural Dynamics*, 29:945–968.
[2] R. DesRoches, M. Delemont. (2002). Seismic retrofit of simply supported bridges using shape memory alloys. *Engineering Structures*, 24:325–332.
[3] J. Ocel, R. DesRoches, R. T. Leon, W. G. Hess, R. Krumme, J. R. Hayes, S. Sweeney. (2004). Steel beam-column connections using shape memory alloys. *Journal of Structural Engineering*, 130(5):732–740.
[4] M. Dolce, D. Cardone, F. C. Ponzo, C. Valente. (2005). Shaking table tests on reinforced concrete frames without and with passive control systems. *Earthquake Engineering and Structural Dynamics*, 34:1687–1717.
[5] V. Torra, A. Isalgue, F. Martorell, P. Terriault, F.C. Lovey. (2007). Built in dampers for family homes via SMA: An ANSYS computation scheme based on mesoscopic and microscopic experimental analyses. *Engineering Structures*, 29:1889–1902.
[6] Y. Zhang, S. Zu. (2007). A shape memory alloy-based reusable hysteretic damper for seismic hazard mitigation. *Smart Materials and Structures*, 16:1603–1623.

[7] D. A. Shook, P. N. Roschke, O. E. Ozbulut. (2008). Superelastic semi-active damping of a base-isolated structure. *Structural Control and Health Monitorig*, 15:746–768.
[8] A. Bhattacharyya, L. Sweeney, Faulkner M. G. (2002). Experimental characterization of free convection during thermal phase transformations in shape memory alloy wires. *Smart Material and Structures*, 11:411–422.
[9] R. Matsui, H Tobushi, T. Ikawa. (2004). Transformation-induced creep and stress relaxation of TiNi shape memory alloy. *Proceedings of the Institution of Mechanical Engineers, Part L: Journal of Materials: Design and Applications*, 218(4):343–353.
[10] M. D. Symans, M. C. Constantinou. (1999). Semi-active control systems for seismic protection of structures: a state-of-the-art review. *Engineering Structures*, 21:469–487.
[11] G. W. Housner, L. A. Bergman, T. K. Caughey, A. G. Chassiakos, R. O. Claus, S. F. Masri, R. E. Skelton, T. T. Soong, B. F. Spencer, J. T. P. Yao. (1997). Structural control. Past, present, and future. *Journal of Engineering Mechanics*, 123(9):897 – 971.
[12] F. Auricchio, R. L. Taylor, J. Lubliner. (1997). Shape-memory alloys: macromodelling and numerical simulations of the superelastic behaviour. *Computer Methods in Applied Mechanics and Engineering*, 146:281–312.
[13] J. McCormick, R. DesRoches, D. Fugazza, F. Auricchio. (2006). Seismic vibration control using superelastic shape memory alloys. *Journal of Engineering Materials and Technology*, 128(3):294–301.
[14] F. Auricchio, D. Fugazza, R. DesRoches. (2006) Numerical and experimental evaluation of the damping properties of shape-memory alloys. *Journal of Engineering Materials and Technology*, 128(3):312–319.
[15] K. Tanaka, S. Kobayashi, Y. Sato. (1986). Thermomechanics of transformation pseudoelasticity and shape memory effect in alloys. *International Journal of Plasticity*, 2:59–72.
[16] C. Liang, C. A. Rogers. (1990). One-dimensional thermomechanical constitutive relations for shape memory materials. *Journal of Intelligent Systems and Structures*, 1:207–234.
[17] Y. Ivshin, T. J. Pence. (1994). A thermomechanical model for a one variant shape memory material. *Journal of Intelligent Material Systems and Structures*, 5(4):455–473.
[18] L. C. Brinson, M. S. Huang. (1996). Simplifications and comparisons of shape memory alloy constitutive models. *Journal of Intelligent Material Systems and Structures*, 7:108–114.
[19] F. Auricchio, E. Sacco. (1997). A one-dimensionalmodel for superelastic shape-memory alloys with different elastic properties between austenite and martensite. *International Journal of Non-Linear Mechanics*, 32(6):1101–1114.
[20] D. P. Koistinen, R. E. Marburger. (1959). A general equation prescribing the extent of the austenite-martensite transformation in pure iron-carbon alloys and plain carbon steels. *Acta Metall*, 7:59–60.
[21] A. Vitiello, G. Giorleo, R. E. Morace. (2005). Analysis of thermomechanical behaviour of Nitinol wires with high strain rates. *Smart Material and Structures*, 14:215–221.
[22] C. Cismasiu, F. P. Amarante dos Santos. (2008). Numerical simulation of superelastic shape memory alloys subjected to dynamic loads. *Smart Materials and Structures*, 17(2):25–36.
[23] F. P. Amarante dos Santos. (2011). *Vibration control with shape-memory alloys in civil engineering structures*. PhD thesis, Faculdade de Ciências e Tecnologia da Universidade Nova de Lisboa.
[24] C. Cismasiu, F. P. Amarante dos Santos. (2010). *Shape Memory Alloys*, chapter Numerical simulation of a semiactive vibration control device based on superelastic shape memory alloy wires, pages 127–154. ISBN: 978-953-307-106-0. Scyio, Publishing, Croatia.
[25] E. W. Collings. (1995). *Materials Properties Handbook: Titanium Alloys*. ASM International.
[26] C. Auguet, A. Isalgue, V. Torra, F.C. Lovey, J.L. Pelegrina. (2008). Metastable effects on martensitic transformation in SMA. Aging problems in NiTi. Journal of Thermal Analysis and Calorimetry, 92(1):63–71.
[27] Z. Moumni, A. Van Herpen, P. Riberty. (2005). Fatigue analysis of shape memory alloys: energy approach. *Smart Materials and Structures*, 14:S287–S292.
[28] S. Miyazaki, T. Imai, K. Otsuka. (1986). Effect of cyclic deformation on the pseudoelasticity characteristics of Ti-Ni alloys. *Metalurgical Transactions A*, 17A:115.
[29] The Pacific Earthquake Engineering Research Center and the University of California. *PEER Strong Motion Database*, http://peer.berkeley.edu/smcat.
[30] F. P. Amarante dos Santos, C. Cismasiu, J. Pamies Teixeira. (2012). Semi-active vibration control device based on superelastic NiTi wires. *Structural Control and Health Monitoring*. doi: 10.1002/stc.1500.